MERAL Publications and Solutions Pvt. Ltd.

Original Article

Applications of the biological properties of *Nymphaea rubra* flower and leaf extracts in developing nanoemulgel-based product

Nakuntwalai Wisidsri[1], Suradwadee Thungmungmee[1*], Khemjira Jarmkom[1], Thisakorn Dumrongphuttidecha[1], Monsicha Khuanekkaphan[1], Surachai Techaoei[1], Warachate Khobjai[2]

[1]Faculty of Integrative Medicine, Rajamangala University of Technology Thanyaburi, Pathum Thani, Thailand. [2]Department of Medical Technology, Faculty of Medicine, Western University, Lam Luk Ka, Pathum Thani, Thailand.

Correspondence: Suradwadee Thungmungmee, Faculty of Integrative Medicine, Rajamangala University of Technology Thanyaburi, Pathum Thani, Thailand. suradwadee_t@rmutt.ac.th

Received: 01 November 2025; **Revised:** 23 February 2026; **Accepted:** 24 February 2026

ABSTRACT

The present study investigated the biological properties of *Nymphaea rubra* Roxb. ex Andrews (*N. rubra*) for their potential as natural active ingredients in nanoemulgel formulation. Water, ethanolic, and methanolic extracts were evaluated for total phenolic content (TPC) and demonstrated antioxidant activities, including their ability to scavenge 2,2-diphenyl-1-picrylhydrazyl (DPPH), 2,2′-azino-bis(3-ethylbenzothiazoline-6-sulfonic acid) (ABTS), and nitric oxide (NO) radicals in vitro, as well as their reducing power through ferric ion (Fe^{3+}) to ferrous ion (Fe^{2+}) conversion. All *N. rubra* extracts also demonstrated anti-inflammatory properties by reducing NO production in lipopolysaccharide (LPS)-stimulated macrophages. Both flower and leaf extracts exhibited notable anti-tyrosinase activity. Cytocompatibility of the *N. rubra* extracts was assessed in epidermal keratinocytes (HaCaT), dermal fibroblasts (BJ), melanocytes (B16F10), and macrophages (RAW264.7) to demonstrate primary safety in cellular. Based on these biological properties, the ethanolic extracts of *N. rubra* flowers and leaves were selected for developing the *N. rubra* nanoemulgel formulation. The resulting nanoemulgel demonstrated favorable physicochemical properties following accelerated stability testing, including stability in appearance, homogeneity, pH, and viscosity, while maintaining TPC. These results suggested that *N. rubra* flower and leaf extracts could serve as natural active ingredients for the development of pharmaceutical and cosmeceutical products.

Keywords: Nymphaea rubra, Antioxidant, Anti-tyrosinase, Anti-inflammatory, Cytocompatibility, Nanoemulgel

Introduction

Oxidative stress, caused by an imbalance between reactive oxygen species (ROS) production and antioxidant defenses, is a key mechanism underlying skin damage and aging [1]. ROS, including reactive oxygen, nitrogen, sulfur, and carbon species such as superoxide anion radical ($O_2^{\bullet-}$), hydroxyl radical ($^{\bullet}OH$), singlet oxygen ($^1O_2$), hydrogen peroxide (H_2O_2), nitric oxide (NO), and peroxynitrite ($ONOO^-$), play a major role in skin oxidative stress. These species are predominantly generated during intracellular metabolic processes, particularly mitochondrial electron transport, in which the incomplete reduction of molecular oxygen leads to their formation [2, 3]. In addition to endogenous production, ROS can be induced by exogenous factors, including ultraviolet (UV) radiation, environmental pollution, and exposure to chemical agents [4, 5].

Access this article online	
Website: www.japer.in	**E-ISSN:** 2249-3379

How to cite this article: Wisidsri N, Thungmungmee S, Jarmkom K, Dumrongphuttidecha T, Khuanekkaphan M, Techaoei S, et al. Applications of the biological properties of *Nymphaea rubra* flower and leaf extracts in developing nanoemulgel-based product. J Adv Pharm Educ Res. 2026;16(1):127-37. https://doi.org/10.51847/X2dtNg6a9I

Excessive ROS production disrupts skin redox homeostasis by overwhelming enzymatic and non-enzymatic antioxidant defenses, leading to oxidative stress that damages lipids, proteins, nucleic acids, and ultimately impairs skin and immune cell functions [6-10]. At the cellular level, oxidative stress-induced senescence in keratinocytes, melanocytes, and fibroblasts contributes to aging-associated pigmentary disorders by disrupting epidermal turnover, dysregulating melanogenesis, and promoting extracellular matrix degradation [11]. In aged skin, the immune cells, macrophages, exhibit reduced phagocytic activity and impaired reparative capacity, contributing to persistent low-grade inflammation and cumulative tissue damage [12, 13]. This chronic inflammatory microenvironment, together with oxidative stress, accelerates extracellular matrix degradation and disrupts the skin barrier. Clinically, these alterations manifest as wrinkles, hyperpigmentation, uneven skin tone, and reduced elasticity [14, 15]. Collectively, these findings highlight the central roles of oxidative stress and inflammation in skin aging and support therapeutic strategies targeting redox imbalance, inflammatory signaling, and skin homeostasis to mitigate age-associated dermatological changes [16, 17].

Nymphaea rubra Roxb. ex Andrews (*N. rubra*) is a perennial aquatic plant in the family Nymphaeaceae, native to tropical and subtropical Asia, including India, Bangladesh, Sri Lanka, Malaysia, and Thailand [18, 19]. Recent studies have indicated its medicinal potential, particularly from flowers and rhizomes. The ethyl acetate fraction of flower extracts exhibited antidiabetic and antidyslipidemic effects, with nuciferine and 10,11-dimethoxy-apomorphine identified as key bioactive compounds [20, 21]. Polysaccharides from carpels demonstrated immunomodulatory activity, while cyclic ion mobility-mass spectrometry revealed over 100 phytoconstituents, including numerous newly identified compounds such as phenolic acids, flavonoids, and terpenoids [22]. Notably, the ethyl acetate fraction shows strong antioxidant activity and inhibitory effects against tyrosinase, α-glucosidase, and elastase [23, 24].

One of the major challenges in cosmetic formulation development is achieving effective delivery and long-term stability of active ingredients. Factors such as poor solubility, susceptibility to degradation during storage, and limited skin penetration often compromise the efficacy of bioactive compounds in topical applications [25, 26]. To address these limitations, advanced delivery systems, such as nanoemulsions, have been developed. Nanoemulgels combine the advantages of nanoemulsions and gel matrices, offering enhanced physicochemical stability, uniform distribution of active ingredients, and improved skin permeation, thereby increasing therapeutic efficacy and overall performance in pharmaceutical and cosmeceutical applications [27-31].

Accordingly, this study was designed to systematically evaluate the biological activities of water, ethanolic, and methanolic extracts from the flowers and leaves of N. rubra, with particular emphasis on their antioxidant, anti-tyrosinase, anti-inflammatory, and cytocompatibility activities. Based on the biological performance of the extracts, selected candidates were subsequently incorporated into a nanoemulgel delivery system. The resulting nanoemulgel formulations were then characterized for their physicochemical properties and biological performance to assess their potential suitability for application in functional topical products.

Materials and Methods

Chemical and reagents

2,2-Diphenyl-1-picrylhydrazyl (DPPH), 2,2′-Azino-bis (3-ethylbenzthiazoline-6-sulfonic acid) (ABTS), 2,4,6-Tris(2-pyridyl)-s-triazine (TPTZ), sodium nitroprusside (SNP), resazurin, and vitamin C (Vit C) were purchased from Sigma-Aldrich, USA. The analytical-grade ethanol, methanol, Potassium persulfate ($K_2S_2O_8$), and dimethyl sulfoxide (DMSO) were purchased from RCI Labscan, Thailand. Dulbecco's Modified Eagle's Medium (DMEM), 0.25% Trypsin-EDTA, fetal bovine serum, 0.4% trypan blue, penicillin, and streptomycin were purchased from Gibco, USA. Griess Reagent kit was purchased from Promega, USA. The cosmetic-grade ingredients, including Tween 80, Span 80, Cetiol LC, Carbopol 940, propylene glycol, triethanolamine, and phenoxyethanol, were purchased from CHEME COSMETICS, Thailand.

N. rubra extract preparation

Flowers and leaves of *N. rubra* were washed, oven-dried at 50 °C for 48 h, and ground into powder. Water extraction was performed at 60 °C, followed by filtration and evaporation at 50 °C to obtain the crude extract. Ethanolic and methanolic extracts were prepared by maceration in 95% solvent with shaking at 250 rpm for 24 h, then filtered and concentrated using rotary evaporation. All extracts were stored at 20 °C until further use.

Determination of the total phenolic content (TPC)

The TPC of *N. rubra* flower and leaf extracts was determined using the Folin-Ciocalteu assay. Briefly, 20 µL of each extract was mixed with 10% Folin-Ciocalteu reagent, incubated for 7 min, and then 7.5% sodium carbonate was added, followed by further incubation for 45 min at room temperature. Absorbance was measured at 765 nm using a microplate reader (BMG LABTECH, Germany). TPC was calculated from a gallic acid standard calibration curve and expressed as mg gallic acid equivalents per gram of dry extract (mg GAE/g).

2,2-diphenyl-1-picrylhydrazyl (DPPH) assay

The antioxidant activities of *N. rubra* flower and leaf extracts were evaluated using the DPPH assay [32, 33]. Briefly, 20 µL of each extract (6.25-100 µg/mL) was mixed with 180 µL of 0.20 mM DPPH and incubated for 30 min at room temperature in the dark. Absorbance was measured at 520 nm using a microplate reader. Vit C and 0.2% DMSO were used as the positive and

negative controls, respectively. The percentage of DPPH radical scavenging activity was calculated using the following equation:

$$\%\text{DPPH scavenging activity} = [(A - B)/A] \times 100 \quad (1)$$

Where A: absorbance of DPPH without extracts; B: absorbance of extract or positive control reacted with DPPH

2,2'-azino-bis (3-ethylbenzothiazoline-6-sulfonic acid) (ABTS) radical scavenging assay

The ABTS radical solution was prepared by mixing 7 mM ABTS with 2.45 mM potassium persulfate (1:1) and incubating in the dark for 16 h. Briefly, 20 µL of the extracts (6.25-100 µg/mL) was mixed with 180 µL of ABTS solution, incubated in the dark for 6 min, and absorbance was measured at 750 nm using a microplate reader [34, 35]. The percentage of ABTS radical scavenging was calculated using the following equation:

$$\%\text{ABTS scavenging activity} = [(A - B)/A] \times 100 \quad (2)$$

Where A: absorbance of ABTS without extracts; B: absorbance of extract or positive control reacted with ABTS

Nitric oxide (NO) scavenging assay

Sodium nitroprusside (SNP) was utilized as the nitric oxide donor [32, 36]. Specifically, 10 mM/L of SNP in a pH 7.4 PBS solution was incubated with 1 mL dissolved *N. rubra* extracts at 6.25-100 µg/mL at 25 °C for 180 min. Approximately 100 L of the resulting solution was withdrawn to react with a Griess Reagent kit, whereby the solution was reacted with 20 µL sulfanilamide for 10 min, and then 20 µL N-1-napthylethylenediamine dihydrochloride was added for another 10 min. The reaction mixture absorbance was measured at 560 nm, and the NO concentrations were determined as the nitrite (NO_2^-) concentrations from the standard curve of a standard nitrite solution. PBS and Vit C were used as the negative and positive controls, respectively.

$$\%\text{NO scavenging activity} = [(A - B)/A] \times 100 \quad (3)$$

Where A: absorbance of SNP without extracts; B: absorbance of extract or positive control reacted with SNP.

Ferric reducing antioxidant power (FRAP) assay

The FRAP assay was performed as previously described [37], with slight modifications. The FRAP reagent was freshly prepared by mixing 300 mM sodium acetate buffer (pH 3.6), 10 mM TPTZ in 40 mM HCl, and 20 mM $FeCl_3$ (10:1:1, v/v/v), and preincubated at 37 °C. Briefly, 20 µL of sample (1 mg/mL) was added to 180 µL of FRAP reagent in a 96-well plate, and absorbance was measured at 593 nm using a microplate reader. $FeSO_4 \cdot 7H_2O$ and distilled water served as the standard and blank, respectively. FRAP value was reported as millimoles of Fe2+ equivalents per milligram of dry extract (mmol Fe2+/mg), with the calibration curve for Fe^{2+}.

Anti-tyrosinase test

The tyrosinase inhibitory activity was assessed using the dopachrome method, with kojic acid serving as the positive control [34, 38]. Mushroom tyrosinase (50 U/mL) in 0.067 M phosphate buffer (pH 6.8) was added to a 96-well plate containing *N. rubra* flower and leaf extracts (6.25-100 g/mL). The reaction was initiated by adding L-DOPA (4.5 mM dissolved in phosphate buffer) and incubated at room temperature for 10 min. Dopachrome formation was measured at 492 nm using a microplate reader. Tyrosinase inhibitory percentage was calculated by the following formula:

$$\%\text{Tyrosinase inhibition} = [(A - B) - (C - D)/(A - B)] \times 100 \quad (4)$$

Where A: absorbance of control without extracts; B: absorbance of the blank control (without the extracts and the tyrosinase enzyme); C: absorbance of the test sample (with the extracts and the tyrosinase enzyme); D: absorbance of the blank sample (with the extracts but without the tyrosinase enzyme)

Cell culture

Keratinocytes (HaCaT), melanocytes (B16F10), fibroblasts (BJ), and macrophages (RAW264.7) were maintained in Dulbecco's Modified Eagle Medium (DMEM) supplemented with 10% fetal bovine serum (FBS) and 1% penicillin-streptomycin. The cells were maintained at 37 °C in a humidified atmosphere containing 5% CO_2. Routine subculturing was performed twice weekly using 0.25% trypsin-EDTA. Only cells with a viability greater than 80%, as determined by 0.4% trypan blue exclusion, were used for the experiments.

Resazurin reduction assay

Cells were seeded into 96-well plates at a density of 2×10^5 cells/mL and incubated for 24 h. After attachment, the cells were treated with various concentrations of *N. rubra* flower and leaf extracts (6.25-100 µg/mL) or 0.2% DMSO (negative control) for an additional 24 h. The treated cells were then incubated with 50 µg/mL resazurin at 37 °C for 4 h. The absorbance was determined at 560 and 600 nm [34, 39-41]. The percentage of cell viability was calculated using the following equation:

$$\%\text{Cell viability} = [(OD_{560} - OD_{600})_A / (OD_{560} - OD_{600})_B] \times 100 \quad (5)$$

Where A: absorbance of extract; B: absorbance of 0.2% DMSO.

Cellular nitric oxide (NO) inhibitory assay

RAW 264.7 cells were seeded at a density of 2×10^5 cells/mL in 96-well plates and pretreated with *N. rubra* flower and leaf extracts (6.25-100 µg/mL) for 24 h at 37 °C. Following pretreatment, the cells were stimulated with 1 g/mL LPS and incubated for an additional 24 h. NO production was quantified by measuring NO_2^- levels in the culture supernatants using a Griess reagent kit. Briefly, 100 µL of each supernatant was mixed with 20 L sulfanilamide for 10 min, followed by 20 L N-1-naphthylethylenediamine dihydrochloride for another 10 min. Absorbance was read at 560 nm, and nitrite concentrations were determined from a standard curve of a standard nitrite solution.

Nanoemulsion and nanoemulgel preparation

Firstly, nanoemulsion bases (NEBs) were prepared by varying the weight ratios of surfactant (Tween 80) and co-surfactant (Span 80), as shown in **Table 1**. In NEB preparation, Tween 80 and Span 80 were weighed and mixed with the oil phase (Cetiol LC) using a magnetic stirrer (IKA C-MAG HS 7, Germany) at 600 rpm for 15 min. Aqueous phase containing propylene glycol and deionized water was then added gradually at a rate of 1 mL/min under stirring at 600 rpm. For the *N. rubra* extract nanoemulsion (NENEs) preparation, 0.10% *N. rubra* flower extract and 0.10% *N. rubra* leaf extract, which are the effective concentrations more than 10 times the IC_{50} of DPPH and tyrosinase inhibitory activities, were dissolved in the mixture of Tween 80, Span 80, and Cetiol LC. Then, the aqueous phase was dropped into the mixture. After adding the full amount of aqueous phase, the mixture continued stirring at 600 rpm for 30 min. The homogeneous formulation, characterized by the smallest particle size and the narrowest polydispersity index (PDI), was selected to develop the *N. rubra* extract nanoemulgel formulations, respectively.

For nanoemulgel preparation, 0.30 %w/w Carbopol 940 was dispersed into the suitable NEB and NENE formulations until homogeneous. Triethanolamine was then added and stirred to form a nanoemulgel. Then, phenoxyethanol was added and mixed well. Finally, *N. rubra* extract nanoemulgel was obtained. The formulations were left for 24 h before characterization.

Formulation characterization

The physicochemical properties of NEBs and NENEs were evaluated immediately after preparation by centrifuging at 3,000 rpm for 5 min to ensure uniformity. Particle size, PDI, zeta potential, and electrical conductivity were analyzed using a nanoparticle analyzer with dynamic light scattering (nanoPartica SZ-100V2 Series, HORIBA, Japan). The samples were diluted with deionized water (1:50) and measured at 25 °C with a scattering angle of 90°. Subsequently, the nanoemulgel base and *N. rubra* extract nanoemulgel were examined for color and phase separation. Additionally, pH and viscosity were measured at 25 °C using a pH meter and a Brookfield viscometer with spindle no. 4, respectively.

Heating-cooling stability test

The nanoemulgel base and *N. rubra* extract nanoemulgel were sealed in glass containers and subjected to accelerated stability testing under alternating storage conditions. Samples were cycled between 4 °C and 45 °C (75% relative humidity) every 24 h for a total of seven cycles. The physicochemical properties, including color, phase separation, pH, viscosity, and TPC, were measured using the method described above. For TPC, the value was obtained from a calibration curve of standard gallic acid and was expressed in mg GAE/g *N. rubra* extract nanoemulgel.

Statistical analysis

Data are expressed as the mean ± standard error of the mean (SEM) from three independent experiments. Statistical comparisons between treatment groups and their respective controls were performed using one-way analysis of variance (ANOVA), followed by Tukey's post hoc test, or by paired *t*-test where appropriate. Statistical analysis was conducted using SPSS software (version 23). *P*-values < 0.05 and < 0.01 were considered statistically significant.

Table 1. Composition (%w/w) of nanoemulsion bases (NEB1–NEB4) and *N. rubra* extract nanoemulsions (NENE1–NENE4)

Formulation	Tween 80	Span 80	Cetiol LC	Deionized water	Propylene glycol	*N. rubra* extracts
NEB1	10.00	-	8.00	77.00	5.00	-
NEB2	10.00	2.00	8.00	75.00	5.00	-
NEB3	10.00	4.00	8.00	73.00	5.00	-
NEB4	10.00	6.00	8.00	71.00	5.00	-
NENE1	10.00	-	8.00	76.80	5.00	0.20
NENE2	10.00	2.00	8.00	74.80	5.00	0.20
NENE3	10.00	4.00	8.00	72.80	5.00	0.20
NENE4	10.00	6.00	8.00	70.80	5.00	0.20

Results and Discussion

N. rubra flower and leaf extraction and total phenolic content

Extraction of *N. rubra* flowers with water, ethanol, and methanol yielded 3.11%, 3.34%, and 1.52%, respectively, while leaves yielded 3.25%, 3.72%, and 1.56%. The highest phenolic content was observed in the ethanolic flower extract and the methanolic leaf extract **(Table 2)**. Previous reports have identified diverse bioactive polyphenols in *N. rubra*, with UHPLC analyses revealing 67 compounds, including 21 major constituents. Ethyl

acetate fractions contained the greatest abundance of active compounds, predominantly gallic acid in flowers and pentagalloylglucose in leaves, which are associated with potent antioxidant and enzyme-inhibitory activities [42-44]. Ultrasonic-assisted extraction optimized by response surface methodology efficiently enriched polyphenols from the leaves, producing extracts with high phenolic and flavonoid contents and strong antioxidant potential [45, 46].

In vitro antioxidant properties

Skin aging is largely driven by oxidative stress, which occurs when ROS overwhelm the capacity of endogenous antioxidant defenses [2, 47]. Consequently, numerous studies have focused on antioxidants as promising strategies to reduce or prevent the detrimental effects of oxidative stress on the skin [48-51]. In particular, plant-derived antioxidants, including flavonoids, polyphenols, carotenoids, and vitamins C and E, have been shown to protect against skin photoaging [52]. These antioxidants mitigate oxidative damage by donating electrons or hydrogen atoms to reactive oxidant species, thereby stabilizing them and preventing further cellular damage [53, 54]. To evaluate the protective potential of natural compounds, antioxidant activity is commonly assessed using multiple assays based on different mechanistic principles. The DPPH and ABTS assays measure the ability of antioxidants to donate electrons or hydrogen atoms to neutralize stable free radicals. In contrast, the NO scavenging assay assesses the capacity to eliminate NO radicals implicated in inflammatory processes. In addition, the FRAP assay determines antioxidant reducing capacity by measuring the conversion of ferric (Fe3+) ions to ferrous (Fe2+) ions [55-58]. In the present study, water, ethanolic, and methanolic extracts of *N. rubra* flowers and leaves exhibited significant antioxidant activities, as demonstrated by DPPH, ABTS, NO scavenging, and FRAP assays as follows;

DPPH oxidant scavenging activity

Among the flower and leaf extracts, the methanolic extracts exhibited the strongest activity, followed by the ethanolic extracts **(Table 2)**. Nevertheless, their activities remained lower than that of Vit C, which was used as the positive control.

ABTS oxidant scavenging activity

All *N. rubra* flower extracts showed ABTS radical scavenging activity comparable to vitamin C, with the methanolic extract being the most potent. Among leaf extracts, the ethanolic and water extracts exhibited the highest activity **(Table 2)**.

NO oxidant scavenging activity

The negative control (PBS) exhibited a high nitrite (NO_2^-) concentration, whereas Vit C, the positive control, effectively suppressed nitrite formation **(Table 2)**. Both *N. rubra* flower and leaf extracts demonstrated NO scavenging activity. The flower extracts showed comparable activity across water, ethanolic, and methanolic extracts, while the ethanolic leaf extract exhibited the strongest NO scavenging effect among the leaf samples.

Ferric reducing antioxidant power (FRAP)

The FRAP assay was used to evaluate antioxidant capacity by measuring the ability of extracts to reduce ferric ions (Fe^{3+}) to ferrous ions (Fe^{2+}) under acidic conditions. Among the flower extracts, the methanolic extract exhibited the highest ferric reducing capacity, followed by the ethanolic and water extracts. A similar trend was observed for the leaf extracts. Vit C, used as the positive control, also demonstrated strong reducing power **(Table 2)**.

Table 2. DPPH, ABTS, NO, and mushroom tyrosinase half maximal inhibitory concentrations (IC_{50}) of *N. rubra* flower and leaf extracts, Vit C, and kojic acid

Compounds	TPC (mg GAE/g)	Antioxidant activities; IC_{50} (µg/mL)			FRAP value (mmol FE/mg)	Anti-tyrosinase activity; IC_{50} (µg/mL)
		DPPH	ABTS	NO		
Vit C	-	17.14±1.03	29.85±0.28	39.56±0.31	1.58±0.13	-
	-	-	-	-	-	48.41 ± 2.72
Flowers						
Water	379.52±6.51	39.91±8.46	30.20±1.30	74.81±5.30	1.82±0.14	92.96 ± 2.75
Ethanolic	403.94±31.71	33.19±1.21	27.73±0.54	72.38±7.68	1.88±0.12	77.24 ± 1.61
Methanolic	391.20±23.89	20.19±1.50	25.32±0.49	72.30±4.81	1.96±0.12	96.74 ± 1.37
Leaves						
Water	140.25±7.18	38.02±0.46	34.88±0.21	77.75±1.70	1.73±0.15	89.66 ± 2.82
Ethanolic	352.35±3.18	32.79±0.85	32.29±5.72	54.65±3.71	1.74±0.16	76.96 ± 2.28
Methanolic	370.60±4.24	25.68±0.15	50.04±2.68	55.71±3.93	1.78±0.12	103.60 ± 5.53

Mushroom tyrosinase inhibitory activity

The inhibitory effects of water, ethanolic, and methanolic extracts of *N. rubra* flowers on mushroom tyrosinase activity are shown in **Table 2**. The flower and leaf ethanolic extracts showed the highest activity. Tyrosinase is the key rate-limiting enzyme involved in melanin biosynthesis and acts in concert with tyrosinase-related proteins (TRP)-1 and TRP-2 to regulate

melanogenesis, particularly under conditions of oxidative stress [59, 60].

Oxidative stress, generated during melanin synthesis and by UV-induced ROS, plays a critical role in melanocyte homeostasis and diseases. Excessive oxidative stress enhances melanogenesis and contributes to hyperpigmentation, while chronic oxidative damage is associated with melanocyte transformation and melanoma progression [7, 61, 62]. Accordingly, tyrosinase inhibition not only regulates melanin overproduction but may also reduce oxidative burden in melanocytes. In this study, flower and leaf extracts of *N. rubra* inhibited tyrosinase activity, supporting their potential for managing hyperpigmentation and improving skin brightness.

Cytocompatibility with keratinocytes, fibroblasts, melanocytes, and macrophages

Cell-based assays provide physiologically relevant and ethical platforms for toxicity screening, with cell viability commonly used as a primary indicator of acute cytotoxicity [63-65]. Cell viability assays demonstrated that water, ethanolic, and methanolic flower and leaf extracts were non-cytotoxic at concentrations of 6.25-100 μg/mL, maintaining viability comparable to untreated controls **(Figures 1a-1d)**. These findings provide preliminary biosafety evidence supporting the cytocompatibility of *N. rubra* extracts for potential practical applications.

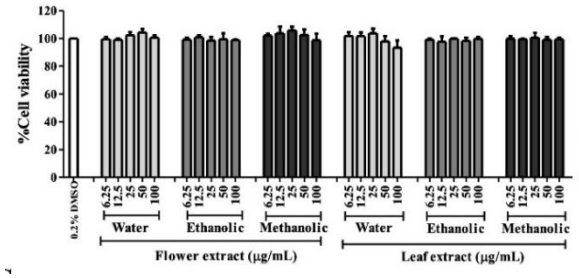

a)

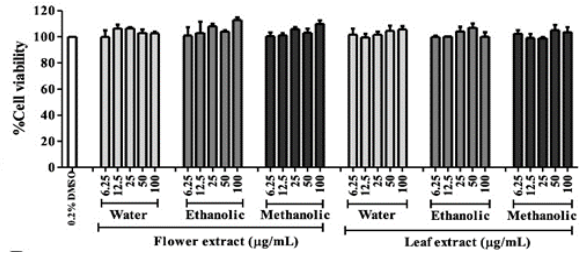

b)

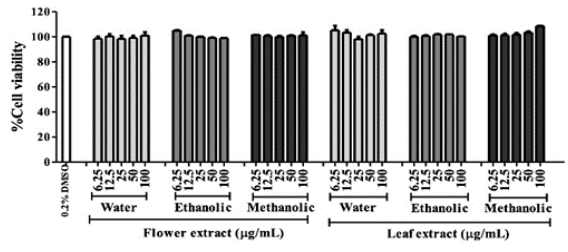

c)

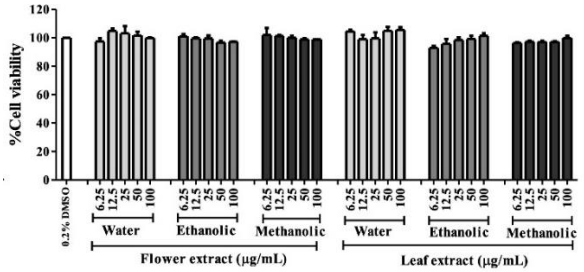

d)

Figure 1. Effect of *N. rubra* flower and leaf extracts on the viability of skin-related cells. a) viability of keratinocytes (HaCaT); b) melanocytes (B16F10); c) fibroblasts (BJ); d) macrophages (RAW264.7). Data from three independent determinations are expressed as mean ± SEM. The statistical significance of the differences was evaluated using a one-way ANOVA followed by Tukey's test.

Anti-inflammatory property

NO is a highly reactive signaling molecule that generates diverse reactive nitrogen species (RNS) depending on oxygen tension, pH, and the surrounding redox milieu. It reacts with superoxide (O_2^-) to form peroxynitrite ($ONOO^-$), a potent oxidant that induces protein nitration and cellular damage. At the same time, other derivatives, including nitrogen dioxide (NO_2) and dinitrogen trioxide (N_2O_3), contribute to oxidative stress and nitrosative modifications. NO can also be oxidized to nitrite (NO_2^-) and nitrate (NO_3^-) or recycled through reductive pathways, reflecting its dual physiological and pathological roles [66].

In the skin, NO is produced by keratinocytes, fibroblasts, endothelial cells, and immune cells, where it regulates physiological processes at basal levels. However, excessive NO generation, primarily via inducible nitric oxide synthase (iNOS) during inflammation, enhances $ONOO^-$ formation and cooperates with cyclooxygenase-2 (COX-2)- prostaglandin E_2 (PGE_2) synthesis to amplify oxidative stress and inflammatory skin disorders [67, 68]. Given its central role in mediating inflammatory responses, modulation of NO production and iNOS activity represents a promising therapeutic strategy for inflammatory and allergic skin diseases [67].

In this study, LPS stimulation markedly increased NO production in RAW264.7 macrophages, whereas untreated cells exhibited lower NO levels. Pretreatment with ethanolic *N. rubra* flower extract (6.25-100 μg/mL) significantly reduced NO levels, while water and methanolic flower extracts were effective at 25-100 μg/mL and 12.5-100 μg/mL, respectively. For leaf extracts, ethanolic and methanolic extracts were active at 6.25-100 μg/mL, whereas the water extract showed inhibition at 50-100 μg/mL **(Figure 2)**.

Accordingly, *N. rubra* flower and leaf extracts effectively scavenged NO radicals generated from the SNP donor and suppressed NO production in activated macrophages. These findings suggest that *N. rubra* extracts may offer protective benefits against inflammatory skin disorders.

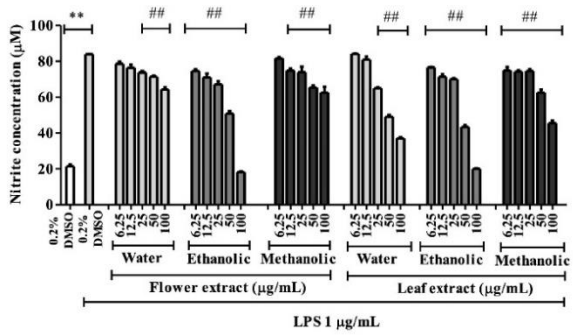

Figure 2. NO inhibitory effects of *N. rubra* flower and leaf extracts. The statistical significance of differences was evaluated by one-way ANOVA followed by Tukey's test. $^{**}p < 0.01$ compared to the non-activated with LPS; $^{\#\#}p < 0.01$ compared to LPS-activated control (0.2%DMSO without extracts).

Characteristics of nanoemulsion and nanoemulgel

To apply the biological activities of *N. rubra* in practical skin applications, ethanolic extracts of the flower and leaves were incorporated into a nanoemulgel system. This advanced topical delivery platform, which incorporates nanoemulsion droplets within a gel matrix, enhances dermal penetration, controlled release, formulation stability, and moisturization, thereby improving therapeutic performance for pharmaceutical and cosmeceutical development [69].

As a result, NEB1, NEB4, NENE1, and NENE4 showed phase separation within 24 h of preparation, whereas the addition of Span 80 as a co-surfactant at 2% (NEB2, NENE2) and 4% (NEB3, NENE3) produced transparent and homogeneous nanoemulsions **(Figure 3a)**. These findings indicate that surfactant and co-surfactant concentrations critically influence nanoemulsion formation and their physicochemical properties, including droplet size, PDI, and stability [70, 71]. The presence of surfactant alone, without a co-surfactant, may be insufficient to reduce interfacial tension, preventing the formation of nanosized droplets and resulting in phase separation (NEB1, NENE1). Conversely, excessive surfactant levels may destabilize the interfacial film, likewise leading to phase separation (NEB4, NENE4).

The physicochemical characteristics of these formulations are summarized in **Table 3**. Particle size, PDI, and zeta potential play a critical role in determining the stability of nanoemulsions [72]. Smaller droplet sizes are associated with reduced surface tension and greater thermodynamic stability. Nanoemulsions with fine droplets enhance solubility and bioactivity by increasing interfacial surface area, thereby improving the absorption of active compounds. A PDI below 0.30 indicates a homogeneous particle size distribution [73]. A high magnitude of surface charge (>30 mV or <−30 mV) enhances electrostatic repulsion between droplets, thereby preventing aggregation and maintaining stable Brownian dispersion. Particle size, PDI, and zeta potential are therefore critical determinants of nanoemulsion physicochemical stability, with NEB3 and NENE3 exhibiting greater stability due to their smaller and more uniform droplet size (~30 nm; PDI 0.28) compared with NEB2 and NENE2. All formulations showed zeta potential values ranging from −45.50±4.29 mV to −44.48±4.78 mV, indicating strong electrostatic stability [73]. Electrical conductivity values ranged from 0.21 to 0.22 mS/cm, exceeding 0.1 mS/cm and confirming that all formulations were oil-in-water nanoemulsions [74].

Based on their favorable physicochemical properties, NEB3 and NENE3 were selected for nanoemulgel development using Carbopol 940 as the gelling agent due to its properties, including enhanced viscosity, optimized rheological behavior, and improved formulation stability without inducing skin irritation [75]. Its incorporation produced a white, opalescent nanoemulgel base and a greenish, opalescent N. rubra extract nanoemulgel, with good miscibility and no phase separation **(Figure 3b and Table 4)**. The extract-loaded formulation exhibited lower pH and viscosity than the base, likely due to the presence of acidic phytochemicals, including gallic acid, caffeic acid, coumaric acid, salicylic acid, protocatechuic acid, and vanillic acid [23]. Nevertheless, both pH and viscosity remained within acceptable ranges for topical application.

Stability of nanoemulgel

The nanoemulgel base and *N. rubra* extract nanoemulgel showed no observable changes in appearance, color, homogeneity, pH, or viscosity throughout the study. In addition, no significant change in total phenolic content was detected after the stability test (117.40±13.53 mg GAE/g) when compared to the starting time (119.77±12.60 mg GAE/g). These results indicate that the formulation remained stable in terms of physicochemical properties and phenolic content under heating-cooling conditions

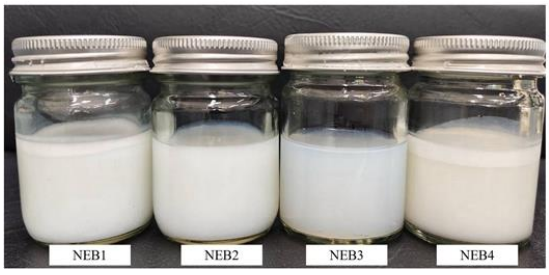

a)

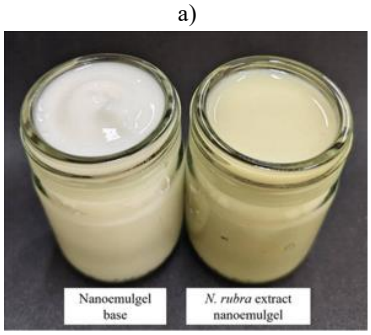

b)

Figure 3. Appearance of nanoemulsion bases: NEB1, NEB2, NEB3, and NEB4. a) Appearance of nanoemulsion bases after 24 h of preparation; b) Appearance of nanoemulgel base and *N. rubra* extract nanoemulgel after 24 h of preparation.

Table 3. Physicochemical properties of nanoemulsion bases (NEB1-NEB4) and *N. rubra* extract nanoemulsions (NENE1-NENE4).

Formulation	Color	Phase separation	Particle size (nm)	Polydisperse index (PDI)	Zeta potential (mV)	Electrical conductivity (mS/cm)
NEB1	White turbid liquid	Yes	ND	ND	ND	ND
NEB2	Slightly turbid liquid	No	128.16±13.38*	0.41±0.05#	−45.14±5.66	0.21±0.00
NEB3	Opalescent liquid	No	30.70 ± 2.64	0.28±0.04	−44.62±8.22	0.21±0.00
NEB4	White turbid liquid	Yes	ND	ND	ND	ND
NENE1	Greenish white turbid liquid	Yes	ND	ND	ND	ND
NENE2	Slightly turbid liquid	No	134.94±11.49**	0.42±0.03##	−44.48±4.78	0.22±0.00
NENE3	Greenish opalescent liquid	No	32.94±0.42	0.28±0.03	−45.50±4.29	0.22±0.00
NENE4	Greenish white turbid liquid	Yes	ND	ND	ND	ND

ND: not determined due to no homogeneous formulation (phase separation).

Data presented are the mean ± standard deviation (n = 3). The statistical significance of the differences was evaluated using a one-way ANOVA followed by Tukey's test. $^{*}p < 0.05$ and $^{**}p < 0.05$ compared to NEB3 and NENE3 for particle size, respectively; $^{\#}p < 0.05$ and $^{\#\#}p < 0.05$ compared to NEB3 and NENE3 for PDI, respectively.

Table 4. Physicochemical properties and total phenolic content (TPC) of nanoemulgel base and *N. rubra* extract nanoemulgel.

Formulation	Color	Phase separation	pH	Viscosity (cP)	TPC (mg GAE/g)
Nanoemulgel base	White opalescent gel	No	5.39±0.05*	16,938.89± 512.02#	-
***N. rubra* extract nanoemulgel**	Greenish opalescent gel	No	5.12±0.02	2,720±74.16	119.77±12.60

Data presented are the mean ± standard deviation (n = 3). The statistical significance of differences was evaluated by one-way ANOVA followed by Tukey's test. $^{*}p < 0.05$ compared to *N. rubra* extract nanoemulgel for pH; $^{\#}p < 0.05$ compared to *N. rubra* extract nanoemulgel for viscosity

Conclusion

In conclusion, *N. rubra* flower and leaf extracts exhibited multifaceted biological activities, including antioxidant, anti-inflammatory, and anti-tyrosinase effects, along with satisfactory cytocompatibility in skin-relevant and immune cell lines, supporting their potential as primary safe and effective natural bioactive ingredients. The incorporation of ethanolic extracts into a nanoemulgel delivery system resulted in a formulation with favorable physicochemical characteristics and good stability under accelerated conditions, while preserving total phenolic content. These findings highlight the suitability of *N. rubra* extracts for nanoemulgel-based pharmaceutical and cosmeceutical applications and provide a scientific basis for their further development as functional ingredients in pharmaceutical and cosmeceutical products. Further studies using advanced biological models are recommended to verify their anti-aging and skin-protective efficacy.

Acknowledgments: The authors would like to thank the Faculty of Integrative Medicine, Rajamangala University of Technology Thanyaburi, for providing the facilities for this research.

Conflict of interest: None

Financial support: This research was supported by the grant of the Plant Genetic Conservation Project, under the Royal initiative of Her Royal Highness Princess Maha Chakri Sirindhorn and the National Science, Research and Innovation Fund, Thailand Science Research and Innovation (TSRI), through Rajamangala University of Technology Thanyaburi (FRB69E1202) (Grant No.: FRB690069/0168).

Ethics statement: None

References

1. Hussen NHa, Abdulla SK, Ali NM, Ahmed VA, Hasan AH, Qadir EE. Role of antioxidants in skin aging and the molecular mechanism of ROS: a comprehensive review. Asp Mol Med. 2025;5:100063.
2. Chen J, Liu Y, Zhao Z, Qiu J. Oxidative stress in the skin: impact and related protection. Int J Cosmet Sci. 2021;43(5):495-509.
3. Kebe IA, Kahl C, Liu Y. The role of transformational leadership in enhancing employee performance: a study of the Vietnamese banking industry. Ann Organ Cult Leadersh Extern Engagem J. 2025;6:21-30. doi:10.51847/g7jtt7Qgxk
4. Papaccio F, A DA, Caputo S, Bellei B. Focus on the contribution of oxidative stress in skin aging. Antioxidants (Basel). 2022;11(6):1121.

5. Guillen J, Pereira R. Institutional influence on gender entrepreneurship in Latin America. Ann Organ Cult Leadersh Extern Engagem J. 2024;5:28-38. doi:10.51847/RaQltcyzXu
6. Liu HM, Cheng MY, Xun MH, Zhao ZW, Zhang Y, Tang W, et al. Possible mechanisms of oxidative stress-induced skin cellular senescence, inflammation, and cancer, and the therapeutic potential of plant polyphenols. Int J Mol Sci. 2023;24(4):3755.
7. Kamiński K, Kazimierczak U, Kolenda T. Oxidative stress in melanogenesis and melanoma development. Contemp Oncol (Pozn). 2022;26(1):1-7.
8. Upadhyay PR, Ho T, Abdel-Malek ZA. Participation of keratinocyte- and fibroblast-derived factors in melanocyte homeostasis, the response to UV, and pigmentary disorders. Pigment Cell Melanoma Res. 2021;34(4):762-76.
9. Zhou H, Wang Y, Li YM, Zheng YW. The potential of macrophages for skin anti-aging. Front Biosci. 2025;30(9):38891.
10. Do DT, Nguyen H, Tran MD, Nguyen NL, Nguyen TBT. An investigation into the factors affecting the effectiveness of SME accountants in Vietnam. Asian J Indiv Organ Behav. 2025;5:19-28. doi:10.51847/U2bKZKQf0a
11. Yang Y, Wu Y, Xiang L, Picardo M, Zhang C. Deciphering the role of skin aging in pigmentary disorders. Free Radic Biol Med. 2025;227:638-55.
12. Lee YI, Choi S, Roh WS, Lee JH, Kim TG. Cellular senescence and inflammaging in the skin microenvironment. Int J Mol Sci. 2021;22(8).
13. Hima N, Benarous D, Louail B, Hamadi W. Impact of social media on consumer purchasing behavior via e-marketing: an empirical study of Algerian university students. Asian J Indiv Organ Behav. 2024;4:49-57. doi:10.51847/v1DRqVmWCg
14. Dan X, Li S, Chen H, Xue P, Liu B, Ju Y, et al. Tailoring biomaterials for skin anti-aging. Mater Today Bio. 2024;28:101210.
15. Lee YT, Tan YJ, Oon CE. An overview of targeted therapy applications in cancer treatment. Asian J Curr Res Clin Cancer. 2025;5(1):30-5. doi:10.51847/P55dZHZAF2
16. Manful CF, Fordjour E, Ikumoinein E, Abbey L, Thomas R. Therapeutic strategies targeting oxidative stress and inflammation: a narrative review. BioChem. 2025;5(4):35.
17. Khan TM, Tahir H, Adil Q, Baig MR, Jaber AAS, Khaliel AM, et al. A three-decade overview of female-specific cancers in Malaysia: a thorough examination. Asian J Curr Res Clin Cancer. 2024;4(2):5-18. doi:10.51847/LIdazW7afN
18. Devi SA, Thongam B, Handique PJ. Nymphaea rubra Roxb. ex Andrews is cultivated as an ornamental, food, and vegetable in the north eastern region of India. Genet Resour Crop Evol. 2015;62(2):315-20.
19. Conti A, Ricci L, Esposito M. In vitro evaluation and in vivo pharmacokinetic assessment of intranasal tadalafil nanocrystals. Ann Pharm Pract Pharmacother. 2025;5:94-111. doi:10.51847/8J1kgy8yW6
20. Ishrat N, Gupta A, Khan MF, Shahab U, Khan MS, Ahmad N, et al. Phytoconstituents of Nymphaea rubra flowers and their anti-diabetic metabolic targets. Fitoterapia. 2024;176:106014.
21. Csep AN, Voiţă-Mekereş F, Tudoran C, Manole F. Understanding and managing polypharmacy in the aging population. Ann Pharm Pract Pharmacother. 2024;4:17-23. doi:10.51847/VdKr0egSln
22. Cheng JH, Lee SY, Lien YY, Lee MS, Sheu SC. Immunomodulating activity of Nymphaea rubra Roxb. extracts: activation of rat dendritic cells and improvement of the TH1 immune response. Int J Mol Sci. 2012;13(9):10722-35.
23. Naznin M, Badrul Alam M, Alam R, Islam S, Rakhmat S, Lee SH, et al. Metabolite profiling of Nymphaea rubra flower extracts using cyclic ion mobility-mass spectrometry and their associated biological activities. Food Chem. 2023;404:134544.
24. Njoroge E, Odhiambo S. Elucidating the therapeutic mechanisms of Agrimonia pilosa Ledeb. extract for acute myocardial infarction via network pharmacology and experimental validation. Pharm Sci Drug Des. 2025;5:48-63. doi:10.51847/eZOWCUj80m
25. Oliveira C, Coelho C, Teixeira JA, Ferreira-Santos P, Botelho CM. Nanocarriers as active ingredients enhancers in the cosmetic industry: the European and North American regulation challenges. Molecules (Basel). 2022;27(5):1669.
26. Snodin DJ, McCrossen SD. Regulatory considerations of pharmaceutical impurities with emphasis on genotoxic impurities. Pharm Sci Drug Des. 2024;4:1-15. doi:10.51847/ck2yogXhAS
27. Raza S, Khan A, Mehmood F, Farooq U. Nationwide implementation of essential pharmacogenomic testing in the Netherlands: a decision-analytic model of lives saved and cost-effectiveness. Spec J Pharmacogn Phytochem Biotechnol. 2025;5:39-49. doi:10.51847/PUWEymkYkk
28. Ganea M, Horvath T, Nagy C, Morna AA, Pasc P, Szilagyi A, et al. Rapid method for microencapsulation of Magnolia officinalis oil and its medical applications. Spec J Pharmacogn Phytochem Biotechnol. 2024;4:29-38. doi:10.51847/UllqQHbfeC
29. Ahmad MZ, Ahmad J, Alasmary MY, Akhter S, Aslam M, Pathak K, et al. Nanoemulgel as an approach to improve the biopharmaceutical performance of lipophilic drugs: contemporary research and application. J Drug Deliv Sci Technol. 2022;72:103420.
30. Altay Benetti A, Tarbox T, Benetti C. Current insights into the formulation and delivery of therapeutic and cosmeceutical agents for aging skin. Cosmetics. 2023;10(2):54.
31. Sghier K, Mur M, Veiga F, Paiva-Santos AC, Pires PC. Novel therapeutic hybrid systems using hydrogels and

nanotechnology: a focus on nanoemulgels for the treatment of skin diseases. Gels (Basel). 2024;10(1):45.
32. Wisidsri N, Thungmungmee S. Radical scavenging and anti-inflammatory properties of pectin from Cissampelos pareira Linn. Walailak J Sci Technol. 2018;16(11):841-50.
33. Petchesi CD, Kozma K, Iuhas AR, Hodisan R, Jurca AD. Co-occurrence of Beckwith-Wiedemann syndrome and familial long QT syndrome type I: a case report. Interdiscip Res Med Sci Spec. 2025;5(1):17-22. doi:10.51847/ihFGrsCY5a
34. Khuanekkaphan M, Khobjai W, Noysang C, Wisidsri N, Thungmungmee S. Bioactivities of Karanda (Carissa carandas Linn.) fruit extracts for novel cosmeceutical applications. J Adv Pharm Technol Res. 2021;12(2):162-8.
35. Zar H, Moore DP, Andronikou S, Argent AC, Avenant T, Cohen C, et al. Principles of diagnosis and treatment in children with acute pneumonia. Interdiscip Res Med Sci Spec. 2024;4(2):24-32. doi:10.51847/4RVz1Zxy4h
36. Yu M, Ma Y, Han F, Gao X. Effectiveness of mandibular advancement splint in treating obstructive sleep apnea: a systematic review. J Curr Res Oral Surg. 2025;5:25-32. doi:10.51847/AInSXrD9rc
37. Youn JS, Kim YJ, Na HJ, Jung HR, Song CK, Kang SY, et al. Antioxidant activity and contents of leaf extracts obtained from Dendropanax morbifera Lev are dependent on the collecting season and extraction conditions. Food Sci Biotechnol. 2019;28(1):201-7.
38. Phewphong S, Roschat W, Jandaruang J, Leelatam T, Arthan S, Poomsuk N, et al. Analysis of volatile organic compounds, antioxidant, tyrosinase inhibitory, and antimicrobial activities of essential oils from citronella grass and kaffir lime. Trends Sci. 2025;22(4):9434.
39. Akaberi M, Emami SA, Vatani M, Tayarani-Najaran Z. Evaluation of antioxidant and anti-melanogenic activity of different extracts of aerial parts of N. sintenisii in murine melanoma B16F10 cells. Iran J Pharm Res. 2018;17(1):225-35.
40. Mickevičius I, Astramskaitė E, Janužis G. A systematic review of the implant success rate following immediate implant placement in infected sockets. J Curr Res Oral Surg. 2024;4:20-31. doi:10.51847/PcPJL1v1XF
41. Yılmazer E, Altinok A. Innovative approaches to delivering mindfulness-based stress reduction (MBSR) in cancer care: improving access and engagement. Int J Soc Psychol Asp Healthc. 2024;4:1-12. doi:10.51847/4u9e1ZvfMS
42. Naznin M, Alam R, Alam MB, Jung MJ, Lee SH, Kim S. Biological activities, identification, method development, and validation for analysis of polyphenolic compounds in Nymphaea rubra flowers and leaves by UHPLC-Q-cIM-TOF-MS and UHPLC-TQ-MS. Phytochem Anal. 2024;35(4):799-816.
43. Dupont H, Lefevre MA. Patient-taught workshop to develop Calgary-Cambridge communication skills in hospital pharmacy residents: implementation and outcomes. Ann Pharm Educ Saf Public Health Advocacy. 2024;4:185-91. doi:10.51847/Z4Tey6oMKA
44. Kowalski TW, Reis LB, Andreis TF, Ashton-Prolla P, Rosset C. Rare co-occurrence of two mutational variants in NF1: molecular testing reveals diagnostic surprises. J Med Sci Interdiscip Res. 2024;4(2):20-9. doi:10.51847/H2qQlZTYO7
45. Elamin SM, Redzuan AM, Aziz SAA, Hamdan S, Masmuzidin MZ, Shah NM. Educational impact on glycemic outcomes among children and adolescents diagnosed with type 1 diabetes. J Med Sci Interdiscip Res. 2023;3(1):41-64. doi:10.51847/s5KgRZ9e1O
46. Naznin M, Alam MB, Lee SH, Kim S. Optimizing ultrasonic-assisted extraction and untargeted metabolite identification from red water lily (Nymphaea rubra) leaves with enhanced antioxidant activity. Food Chem Adv. 2024;4:100696.
47. Rinnerthaler M, Bischof J, Streubel MK, Trost A, Richter K. Oxidative stress in aging human skin. Biomolecules. 2015;5(2):545-89.
48. Budzianowska A, Banaś K, Budzianowski J, Kikowska M. Antioxidants to defend healthy and youthful skin: current trends and future directions in cosmetology. Appl Sci. 2025;15(5):2571.
49. Mukherjee S, Chopra H, Goyal R, Jin S, Dong Z, Das T, et al. Therapeutic effect of targeted antioxidant natural products. Discov Nano. 2024;19(1):144.
50. Hoang HT, Moon JY, Lee YC. Natural antioxidants from plant extracts in skincare cosmetics: recent applications, challenges, and perspectives. Cosmetics. 2021;8(4):106.
51. Pardo-Zamora F, Castellano-Rioja G. Liquid biopsy in oral cancer diagnosis: a narrative review of emerging diagnostic tools. Arch Int J Cancer Allied Sci. 2024;4(1):1-6. doi:10.51847/CcaLqtzvoN
52. Petruk G, Del Giudice R, Rigano MM, Monti DM. Antioxidants from plants protect against skin photoaging. Oxid Med Cell Longev. 2018;2018:1454936.
53. Chaudhary P, Janmeda P, Docea AO, Yeskaliyeva B, Abdull Razis AF, Modu B, et al. Oxidative stress, free radicals and antioxidants: potential crosstalk in the pathophysiology of human diseases. Front Chem. 2023;11:1158198.
54. Maslyakova AR, Magomedova SA, Romantsov IN, Nurbagandov SM, Bulovin MN, Podobin OR. Evaluation of the anticancer potential of selenium nanoparticles. Arch Int J Cancer Allied Sci. 2023;3(2):41-7. doi:10.51847/POXX7HfEZo
55. Munteanu IG, Apetrei C. Analytical methods used in determining antioxidant activity: a review. Int J Mol Sci. 2021;22(7):3380.
56. Zhang Y, Pan A, Wang J, Pan X, Chen J, Li H, et al. Assessing the role of play therapy in easing anxiety and despair in children with cancer. Int J Soc Psychol Asp Healthc. 2023;3:40-8. doi:10.51847/S7vZ2lgmuc
57. Jagsi R, Lee J, Roselin D, Ira K, Williams J. Do U.S. medical schools follow medical associations'

recommendations on paid parental leave for faculty? Ann Pharm Educ Saf Public Health Advocacy. 2025;5:1-11. doi:10.51847/r117In8wdi

58. Bibi Sadeer N, Montesano D, Albrizio S, Zengin G, Mahomoodally MF. The versatility of antioxidant assays in food science and safety chemistry, applications, strengths, and limitations. Antioxidants (Basel). 2020;9(8):709.
59. Pillaiyar T, Manickam M, Namasivayam V. Skin whitening agents: medicinal chemistry perspective of tyrosinase inhibitors. J Enzyme Inhib Med Chem. 2017;32(1):403-25.
60. Salem HM, Watanabe S, Chang AH. Ethical concerns in managing anorexia nervosa: a content analysis of ethics consultation records. Asian J Ethics Health Med. 2025;5:25-35. doi:10.51847/oHEI6FgL3V
61. Leadbeatter D, Tjaya KC. Human rights and bioethical principles in correctional settings: a systematic review of the evidence. Asian J Ethics Health Med. 2024;4:97-106. doi:10.51847/wSNBedLrGt
62. Al-Mubarak AM, Alkhaldi FA, Alghamdi AA, Almahmoud MA, Alghamdi FA. Awareness and clinical competency of dental students in crown lengthening procedures. Asian J Periodontics Orthod. 2024;4:42-51. doi:10.51847/r5cLVpz1UT
63. Jiang M, Chattopadhyay AN, Rotello VM. Cell-based chemical safety assessment and therapeutic discovery using array-based sensors. Int J Mol Sci. 2022;23(7):3672.
64. Xia Y, Wang WX. Development and application of cell-based bioassay in aquatic toxicity assessment. Aquat Toxicol. 2025;285:107427.
65. Bona C, Camacho-Alonso F, Vaca A, Llorente-Alonso M. Oral biofilm control in patients using orthodontic aligners: evidence from a systematic review. Asian J Periodontics Orthod. 2025;5:33-42. doi:10.51847/silhUaqfip
66. Martemucci G, Costagliola C, Mariano M, D'Andrea L, Napolitano P, D'Alessandro AG. Free radical properties, source and targets, antioxidant consumption, and health. Oxygen. 2022;2(2):48-78.
67. Kim JH, Choi MS. Nitric oxide signal transduction and its role in skin sensitization. Biomol Ther (Seoul). 2023;31(4):388-94.
68. Salvemini D, Kim SF, Mollace V. Reciprocal regulation of the nitric oxide and cyclooxygenase pathway in pathophysiology: relevance and clinical implications. Am J Physiol Regul Integr Comp Physiol. 2013;304(7):R473-87.
69. Donthi MR, Munnangi SR, Krishna KV, Saha RN, Singhvi G, Dubey SK. Nanoemulgel: a novel nanocarrier as a tool for topical drug delivery. Pharmaceutics. 2023;15(1):164.
70. Thungmungmee S, Wisidsri N. Protective effects of avocado peel and seed extracts against UVB-damaged fibroblasts for the development of an anti-photoaging nanoemulgel. Sci Rep. 2025;15(1):28006.
71. Algahtani MS, Ahmad MZ, Ahmad J. Investigation of factors influencing formation of nanoemulsion by spontaneous emulsification: impact on droplet size, polydispersity index, and stability. Bioengineering (Basel). 2022;9(8):384.
72. Li H, Tan X, Qin L, Gatasheh MK, Zhang L, Lin W, et al. Preparation, process optimisation, stability, and bacteriostatic assessment of composite nanoemulsion containing corosolic acid. Heliyon. 2024;10(19):e38283.
73. Pham KQC, Lieu L, Le Tan NT, Nguyen TB, To TT, Nguyen LMD, et al. A comparison of sonication and phase inversion temperature methods for formulating lavender essential oil nanoemulsions: stability, antioxidant capacity, and industrial potential. Trends Sci. 2025;22(5):9428.
74. Ali FR, Shoaib MH, Yousuf RI, Ali SA, Imtiaz MS, Bashir L, et al. Design, development, and optimization of dexibuprofen microemulsion-based transdermal reservoir patches for controlled drug delivery. Biomed Res Int. 2017;2017:4654958.
75. Fenny Indah S, Desy N, Dina F, editors. Overview: application of Carbopol 940 in gel. In: Proceedings of the International Conference on Health and Medical Sciences (AHMS 2020). Paris: Atlantis Press; 2021.